

Na⁺,K⁺-ATPase Functionally Interacts with the Plasma Membrane Na⁺,Ca²⁺ Exchanger to Prevent Ca²⁺ Overload and Neuronal Apoptosis in Excitotoxic Stress

Dmitry A. Sibarov, Artemiy E. Bolshakov, Polina A. Abushik, Igor I. Krivoi, and Sergei M. Antonov

Sechenov Institute of Evolutionary Physiology and Biochemistry, Russian Academy of Sciences, St. Petersburg, Russia (D.A.S., A.E.B., P.A.A., S.M.A.); Department of General Physiology, St. Petersburg State University, St. Petersburg, Russia (I.I.K.); and Laboratory of Molecular Neurodegeneration, St. Petersburg State Polytechnic University, St. Petersburg, Russia (D.A.S., P.A.A., S.M.A.)

Received July 11, 2012; accepted August 24, 2012

ABSTRACT

Using a fluorescent viability assay, immunocytochemistry, patch-clamp recordings, and Ca²⁺ imaging analysis, we report that ouabain, a specific ligand of the Na⁺,K⁺-ATPase cardiac glycoside binding site, can prevent glutamate receptor agonist-induced apoptosis in cultured rat cortical neurons. In our model of excitotoxicity, a 240-min exposure to 30 μM *N*-methyl-D-aspartate (NMDA) or kainate caused apoptosis in ~50% of neurons. These effects were accompanied by a significant decrease in the number of neurons that were immunopositive for the antiapoptotic peptide Bcl-2. Apoptotic injury was completely prevented when the agonists were applied together with 0.1 or 1 nM ouabain, resulting in a greater survival of neurons, and the percentage of neurons expressing Bcl-2 remained similar to those obtained without agonist treatments. In addition, subnanomolar concentrations of ouabain prevented the increase of spontaneous excitatory postsynaptic current's frequency and the intracellular Ca²⁺ overload induced by excitotoxic insults.

Loading neurons with 1,2-*bis*(2-aminophenoxy)ethane-*N,N,N',N'*-tetraacetic acid or inhibition of the plasma membrane Na⁺,Ca²⁺-exchanger by 2-(2-(4-(4-nitrobenzyloxy)phenyl)ethyl)isothiurea methanesulfonate (KB-R7943) eliminated ouabain's effects on NMDA- or kainite-evoked enhancement of spontaneous synaptic activity. Our data suggest that during excitotoxic insults ouabain accelerates Ca²⁺ extrusion from neurons via the Na⁺,Ca²⁺ exchanger. Because intracellular Ca²⁺ accumulation caused by the activation of glutamate receptors and boosted synaptic activity represents a key factor in triggering neuronal apoptosis, up-regulation of Ca²⁺ extrusion abolishes its development. These antiapoptotic effects are independent of Na⁺,K⁺-ATPase ion transport function and are initiated by concentrations of ouabain that are within the range of an endogenous analog, suggesting a novel functional role for Na⁺,K⁺-ATPase in neuroprotection.

Introduction

Ionotropic glutamate receptors (GluRs) are critically involved in physiological processes in the mammalian central

nervous system (CNS), including generation of neuronal activity patterns (Iwasato et al., 2000) and learning and memory (Bliss and Collingridge, 1993; Tang et al., 1999). Functional deregulation of neuronal metabolism resulting from an overactivation of GluRs leads to neuronal death and underlies a variety of CNS disorders including stroke, neurodegenerative diseases, and spinal cord and brain injuries (Choi, 1988; Olney, 1994; Lipton, 1999). The prolonged presence of glutamate released from neurons and glial cells by nonquantal secretion (Rossi et al., 2000) and activation of GluRs have extensive consequences for neuron

This work was supported by the Russian Foundation for Basic Research [Grants 08-04-00423, 11-04-00397 (to S.M.A.); 10-04-00970 (to I.I.K.)]; the Russian Federation Ministry of Education and Science [Contract 8476] (to IEPH RAS); and Saint-Petersburg State University [Research Grant 1.37.118.2011] (to I.I.K.).

Article, publication date, and citation information can be found at <http://jpet.aspetjournals.org>.
<http://dx.doi.org/10.1124/jpet.112.198341>.

ABBREVIATIONS: GluR, ionotropic glutamate receptor; AM, acetoxymethyl ester; ANOVA, analysis of variance; AWCE, alternative to GluR ways of Ca²⁺ entry; AMPAR, 2-amino-3-(5-methyl-3-oxo-1,2-oxazol-4-yl)propanoic acid receptor; AO, acridine orange; BAPTA, 1,2-*bis*(2-aminophenoxy)ethane-*N,N,N',N'*-tetraacetic acid; [Ca²⁺]_i, intracellular calcium concentration; CNS, central nervous system; EB, ethidium bromide; EPSC, excitatory postsynaptic current; sEPSC, spontaneous EPSC; FVA, fluorescent viability assay; I-V, current-voltage; KA, kainic acid; KAR, KA receptor; KB-R7943, 2-(2-(4-(4-nitrobenzyloxy)phenyl)ethyl)isothiurea methanesulfonate; MK-801, (+)-5-methyl-10,11-dihydro-5*H*-dibenzo[*a,c'*]cyclohept-5,10-imine; NCX, Na⁺/Ca²⁺ exchanger; NKA, Na⁺,K⁺-ATPase; NMDA, *N*-methyl-D-aspartate; NMDAR, NMDA receptor; Ouab, ouabain molecule; PBS, phosphate-buffered saline.

functioning. These consequences start with intracellular Ca²⁺ overload, imbalance of transmembrane ion gradients, and activation of various intracellular cascades and end with the destruction of the plasma membrane or nuclear apparatus of neurons (Choi, 1987, 1988; Olney, 1994; Green and Reed, 1998; Kidd, 1998). Massive cytoplasmic Ca²⁺ accumulation is thought to be one of the most important triggers of various cell death mechanisms, usually ending as apoptosis (Khodorov, 2004). Apoptosis, or programmed cell death, plays an enormous role in the development and formation of organs, as well as in the functioning of rapidly renewing tissues (Johnston, 1994) and is the key factor in neuronal pathogenesis and necrosis (Choi, 1988; Olney, 1994; Lipton, 1999; Khodorov, 2004).

Similar neuronal dysfunction and neurodegeneration are induced by micromolar concentrations of ouabain, a specific inhibitor of Na⁺,K⁺-ATPase (Xiao et al., 2002). Na⁺,K⁺-ATPase sets the cellular ion gradients for K⁺ and Na⁺ by active transport, thereby providing the driving force for membrane excitability and many other transporters and exchangers. It is now recognized that Na⁺,K⁺-ATPase, in addition to its primary role as an ion transporter, can function as a receptor signaling molecule. The extracellular loops of the catalytic α -subunit of Na⁺,K⁺-ATPase form a binding site that is the only known, highly specific receptor for ouabain and other cardiotonic steroids (Ogawa et al., 2009; Lingrel, 2010) and their circulating endogenous analogs (Blaustein, 1993; Schoner and Scheiner-Bobis, 2007; Bagrov and Shapiro, 2008). Upon binding of ouabain to this receptor, Na⁺,K⁺-ATPase interacts with neighboring membrane proteins to affect diverse cell functions such as protein synthesis, proliferation, cell differentiation, gene expression, regulation of intracellular Ca²⁺, contractile properties, synaptic efficacy, and neural differentiation (Xie and Askari, 2002; Krivoi et al., 2006; Aperia, 2007; Hazelwood et al., 2008; Desfrere et al., 2009; Li and Xie, 2009; Radzyukevich et al., 2009; Rose et al., 2009; Heiny et al., 2010). In addition, ouabain in nanomolar concentrations stimulates the reversed mode of plasma membrane Na⁺,Ca²⁺ exchange in snail neurons (Saghian et al., 1996).

Whereas ouabain, as an endogenous agent, has been found in subnanomolar concentrations in rat blood plasma and cerebrospinal fluid (Blaustein, 1993; Dobretsov and Stimers, 2005; Schoner and Scheiner-Bobis, 2007; Bagrov and Shapiro, 2008), its functional relevance for CNS is not clearly understood. Previously, antiapoptotic action of low ouabain doses was described when kainic acid (KA) and ouabain were injected into the rat brain in vivo (Golden and Martin, 2006). Here, we investigate the pharmacological effects of ouabain in a wide range of concentrations (0.01 nM to 30 μ M) in vitro on cortical neurons in primary culture under normal conditions and excitotoxic stress. Neuronal viability is also tested in the presence of digoxin, another highly specific ligand of Na⁺,K⁺-ATPase (Katz et al., 2010). We examine the possibility that Na⁺,K⁺-ATPase can interact with the signaling pathways involved in neuronal injury triggered by GluR (NMDAR, AMPAR, and KAR subtypes) overactivation and, moreover, may antagonize neurodegeneration. Using a fluorescent viability assay (FVA) with confocal microscopy and immunocytochemistry we demonstrate that ouabain at subnanomolar concentrations prevents rat cortical neuron apoptosis during GluR agonist-induced stress. Based on our

patch-clamp and Ca²⁺ imaging experiments, this neuroprotective antiapoptotic effect of ouabain results from the up-regulation of Ca²⁺ extrusion mechanisms and involves the plasma membrane Na⁺,Ca²⁺ exchanger (NCX).

Materials and Methods

Preparation and Solutions. Cell cultures were prepared as described previously (Antonov et al., 1998; Mironova et al., 2007). All procedures using animals were in accordance with recommendations of the Federation for Laboratory Animal Science Associations and approved by the local Institutional Animal Care and Use Committees. Wistar rats (provided by the Sechenov Institute's Animal Facility) 16 days pregnant (26 animals in this study) were sacrificed by CO₂ inhalation. Fetuses (10–15) were removed, and their cerebral cortices were isolated, enzymatically dissociated, and used to prepare primary neuronal cultures. Cells were used for experiments after 7 to 15 days in culture (Mironova et al., 2007; Han and Stevens, 2009). Experiments were performed at room temperature (20–23°C).

Neuronal cultures were perfused by the indicated concentrations of drugs dissolved in the bathing solutions. The principal external bathing solution consisted of 140 mM NaCl, 2.8 mM KCl, 1.0 mM CaCl₂, 1.0 mM MgCl₂, and 10 mM HEPES. The content of the external solution slightly varied depending on the purpose of the experiments. In experiments with *N*-methyl-D-aspartate (NMDA), Mg²⁺ was omitted from the bathing solution, because it blocks the channels of NMDARs (Nowak et al., 1984). The pH of each external solution was adjusted to 7.4 with NaOH.

Recordings of integral cellular currents were done by using whole-cell configurations of the patch-clamp technique. In most of the experiments, pipettes were filled with a solution containing 9 mM NaCl, 17.5 mM KCl, 121.5 mM K-gluconate, 1 mM MgSO₄, 10 mM HEPES, 0.2 mM EGTA, 2 mM MgATP, and 0.5 mM NaGTP (Han and Stevens, 2009). In some ramp experiments 0.5 μ M tetrodotoxin was added to the external solution, and Cs⁺ intracellular pipette solution was used to increase noise resolution and stability of whole-cell recording within a wide range of membrane voltage by blocking K⁺ channels. Substitution of Cs⁺ for K⁺ in pipette solution does not affect either the kinetics or conductance of GluR channels (Antonov et al., 1995, 1998; Traynelis et al., 2010). The Cs⁺ pipette solution contained 120 mM CsF, 10 mM CsCl, 10 mM EGTA, and 10 mM HEPES. The pH was adjusted to 7.4.

Excitotoxic Insults. Directly before the experiments, coverslips with neuronal cultures were placed in the bathing solution. To trigger necrotic cell injury and apoptosis 30 μ M NMDA (30 μ M glycine was present as a coagonist of NMDAR; Johnson and Ascher, 1987) or 30 μ M KA was added to the bathing solution. When the effects of ouabain or digoxin were studied, the compounds were applied alone or in combination with the glutamate receptor agonists. Neuronal cultures were subjected to FVA and immunocytochemistry after 240 min of continuous presence of the compounds. In some experiments the effects of longer treatments (360 min) were studied.

Quantification of Cell Viability. In FVA cell viability (Mironova et al., 2007) was determined from fluorescent images by quantification of fluorescence after staining all nuclei with acridine orange (AO) and staining dead cell nuclei with ethidium bromide (EB). First, cells were treated with 0.001% AO for 30 s. After complete washout of contaminating AO, cells were exposed to 0.002% EB for 30 s. This procedure was applied directly before every measurement. AO readily permeates the plasma membrane, stains the nuclei of neurons, and emits a green fluorescence in live neurons; however, it undergoes a red emission shift in apoptotic nuclei (orange spectrum) (Zelenin, 1966). EB (red fluorescence) is normally impermeable and enters the nuclei of necrotic cells when the plasma membrane is compromised. As a result, in fluorescent images the nuclei of live neurons, labeled with AO, looked green and the nuclei of injured neurons, labeled with EB, looked red. In the absence of colocalized

pixels cell viability was estimated by the ratio of green pixels (the number) to the total number of fluorescent pixels (red plus green). If some neurons exhibited apoptotic transformations their nuclei looked yellow-orange, revealing colocalization of fluorescence in the green and red spectral regions. In this case, the fractions of live, apoptotic, and necrotic cells were calculated on the basis of correlation plot as the ratio of green, yellow-orange, and red pixels to the total number of fluorescent pixels (the sum of green, yellow-orange, and red), correspondingly.

Immunohistochemistry. The antiapoptotic peptide Bcl-2 was visualized immunochemically by using rabbit polyclonal antibodies and secondary antibodies conjugated with *R*-phycoerythrin on fixed cultures. Cells were fixed with 4% paraformaldehyde solution in phosphate-buffered saline (PBS) for 30 min. After fixation, cells were washed twice with PBS (15 min \times 2). Before treatment with 2% bovine serum albumin, cells were incubated with 0.2% Triton X-100 for 15 min, washed with PBS, and exposed to primary antibodies for 12 h at 4°C. After washing to remove primary antibodies, fluorochrome-conjugated secondary antibodies were added. Reactions with secondary antibodies lasted for 40 min at room temperature (23°C). Before data were recorded, coverslips with antibody-bound preparations were pasted on slides with Moviol glue to prevent the fading of fluorochromes.

Imaging and Image Processing. Fluorescence images were captured by using a Leica SP5 MF scanning confocal microscope (inverted) (Leica Microsystems, Inc., Bannockburn, IL). Cultures were viewed with 20 \times (HCX APO CS 20 \times /0.70; Leica Microsystems, Inc.) or 63 \times (HCX APO CS 63 \times /1.4; Leica Microsystems, Inc.) immersion objectives. To resolve fine details an additional electronic zoom with a factor of 1.5 to 3.5 was used. Fluorochromes were excited with a 488-nm laser line. Images were captured in the green and red parts of the spectrum (for the FVA) and the red spectral region (for phycoerythrin). To improve signal-to-noise ratio six scans (512 \times 512 pixel array) were averaged at each optical section. Some areas of neuronal culture contained glia, forming a thin, flat layer subjacent to neuronal bodies bulging out above. To exclude glia from images, we set confocal optical section (for 63 \times objective the thickness of optical section was 0.4 μ m) to cross neuronal bodies only. Transmitted light images were also captured to verify the correct position of the focal plane by using morphological criteria.

For two-channel imaging of AO and EB emission, the emitted fluorescence was acquired at 500 to 560 nm (green region of spectrum for AO) and >600 nm (red region of spectrum for EB) and collected simultaneously by using separate photo multiplier tubes. Microscope settings were adjusted so that imaging conditions for both channels were kept equal and constant. The confocal images from both channels were merged by using standard Leica Microsystems, Inc. software and ImageJ software (<http://rsbweb.nih.gov/ij/>). Images were processed in ImageJ software by using a custom-written plug-in (<http://sibarov.ru/index.php?slab=software>). The noise threshold value was determined automatically by using the ISO-DATA algorithm implemented in ImageJ. To quantify colocalized and noncolocalized fluorescence correlation plots, which sort values of given pixels in the first image as the *x*-coordinate and values of corresponding pixels in the second image as the *y*-coordinate, images were generated for each measurement. On the resulting image noncolocalized pixels looked green and red and were attributed to live and necrotic neurons, respectively. Pixels with colocalized green and red fluorescence looked yellow-orange and were attributed to the nuclei of apoptotic neurons.

Patch-Clamp Recording. Patch-clamp recordings were carried out on the stage of an inverted microscope (Diaphot TMD; Nikon, Tokyo, Japan) with Hoffman modulation contrast optics. Patch pipettes (2–4 M Ω) were pulled from 1.5-mm (outer diameter) borosilicate standard wall capillaries with inner filament (Sutter Instrument Company, Novato, CA). Recordings were made by using a MultiClamp 700B amplifier (Molecular Devices, Sunnyvale, CA). Whole-cell currents were recorded at membrane voltage of –70 mV

during bath perfusion of 30 μ M NMDA + 30 μ M glycine or 30 μ M KA applied by using a multibarrel perfusion system. Continuous recordings of spontaneous excitatory postsynaptic currents (sEPSCs) were low-pass filtered at 1.5 kHz and digitized at 20 kHz with DigiData 1440A and pClamp 10 software (Molecular Devices). To analyze current-voltage (I-V) relationships, 2-s-long, voltage ramp (from –100 to +30 mV) protocols were applied at the steady-state currents under control conditions and in the presence of GluR agonists. The I-V relationships of NMDA- or KA-induced conductance were then obtained by subtraction of the control ramp current from those in the presence of GluR agonists. Ramp recordings were low-pass filtered at 100 Hz and digitized at 1000 Hz.

Loading of AM Esters and Ca²⁺ Imaging. Cells were loaded with BAPTA AM (2 and 5 μ M), Fluo-3 AM (4 μ M), and Fura-2 AM (10 and 20 μ M) by using conventional protocols. In brief, neuronal cultures were incubated with the AM esters, and 0.02% Pluronic F-127 was added to the external solution for 45 min in the dark at 20 to 23°C. Then, the AM esters were washed out, and cells were incubated in the external solution for another 30 min. For Fluo-3 experiments coverslips with loaded cultures were placed in the perfusion chamber that was mounted on the stage of a Leica SP5 MF inverted microscope. Fluorescence was activated with 488-nm laser light. Images were captured every minute during 60-min experiments. For Fura-2 the perfusion chamber with neuronal culture was mounted on the stage of a Nikon TMS inverted epifluorescence microscope equipped with a 300-W xenon lamp (Intracellular Imaging Inc., Cincinnati, OH) and 30 \times dry objective (Nikon). Cells were visualized with a high-resolution digital black/white charge-coupled device camera (Cohu 4910; Cohu Electronics, Poway, CA), and [Ca²⁺]_i was estimated by the 340/380 ration method, using a *K*_d value of 315 nM for 23°C. Data were analyzed with InCytIm2 (Intracellular Imaging and Photometry System, Cincinnati, OH) and Excel (Microsoft, Redmond, WA).

Drugs. Rabbit polyclonal antibodies for Bcl-2 and secondary antibodies conjugated with *R*-phycoerythrin were purchased from Abcam Inc. (Cambridge, MA). Fura-2 AM was from Fluka (Buchs, Switzerland), Fluo-3 AM was from MoBiTec (Göttingen, Germany), and Pluronic F-127 was from Molecular Probes (Carlsbad, CA). Other compounds were from Sigma-Aldrich (St. Louis, MO). Stock solutions of 10 mM NMDA, 10 mM glycine, and 10 mM KA dissolved in distilled water were stored frozen and thawed on the day of use. Stock solutions with ouabain dissolved in distilled water and digoxin dissolved in ethanol at concentrations of 10 μ M and 1 mM, respectively, were stored refrigerated. Stock solutions of 10 mM BAPTA AM, 10 mM Fura-2 AM, and 10 mM Fluo-3 AM dissolved in dimethyl sulfoxide were stored frozen. All drugs were diluted in the external solution to the indicated concentrations before use.

Statistics. Quantitative data are expressed as means \pm S.E.M. Student's two-tailed *t* tests, ANOVA, Tukey's, and Bonferroni multiple comparison methods were used for statistical analysis. Number of experiments is indicated by *n* throughout. The data were considered as significantly different based on a confidence level of 0.05.

Results

Neuroprotective, Antiapoptotic Effects of Subnanomolar Ouabain in Excitotoxic Insults. Experiments were performed on cultured cortical neurons by using a microscopy-based viability assay that rapidly detects and counts the proportion of live, necrotic, and apoptotic neurons (FVA) (Mironova et al., 2007). The neurons were dual-stained with acridine orange and ethidium bromide. A correlation plot of the intensity of green versus red fluorescence revealed the proportion of live, apoptotic, and necrotic cells.

Under control conditions, when neurons were perfused with the bathing solution, the majority of nuclei remained green (viable) for up to 240 min (Fig. 1A). The image corre-

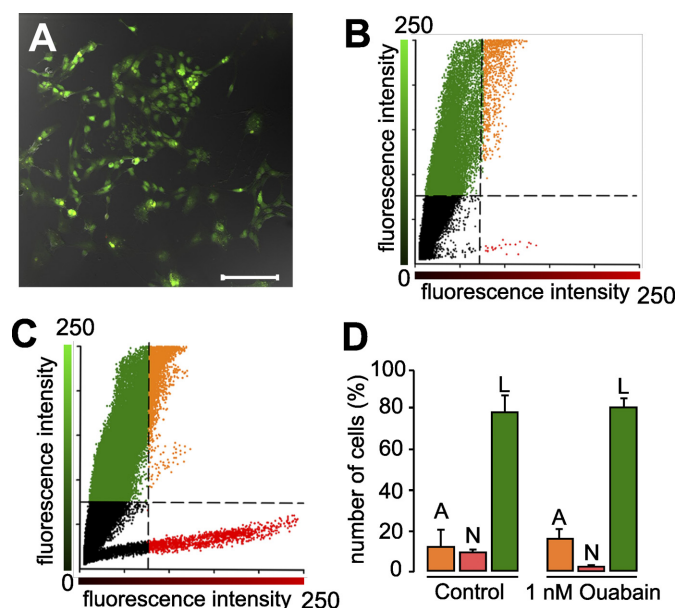


Fig. 1. Ouabain at 1 nM concentration does not induce neurodegeneration. **A**, confocal image represents an overlay of images recorded in green and red spectral regions and in transmitted light (differential interference contrast) of rat cortical neurons after 240-min perfusion with the bathing solution (the control conditions) obtained with the FVA. Scale bar, 100 μ m. **B**, the correlation plot for the image presented in **A**. Most of the fluorescence belongs to the green spectral region, suggesting that a majority of neurons are live. Cell viability (the proportion of live neurons) is 97%; 3% of neurons reveal apoptosis. **C**, the correlation plot for neurons after 240-min exposure to 1 nM ouabain. The majority of fluorescence belongs to the green spectral region. Cell viability is 95%; 4% of neurons reveal apoptosis, and 1% died by necrosis. In both correlation plots the dashed lines indicate thresholds to separate visible fluorescence from dark pixels. **D**, quantitative comparison of the data obtained under control conditions and in the presence of 1 nM ouabain. A, N, and L are the percentages of apoptotic, necrotic, and live neurons, respectively. Measurements in each data pair (for apoptosis, necrosis, and live neurons) are not significantly different ($p > 0.6$; two-tailed Student's t test; $n = 8$).

lation analysis (Fig. 1B) showed that the majority of cells mapped in the region of strong green fluorescence (live) and did not colocalize with the few cells showing low red fluorescence. This indicates that the majority of cells were vital with an intact plasma membrane. Only a small number of nuclei showed a shift in the acridine orange fluorescence to the red spectral region, indicating that these cells were starting to undergo apoptosis. It is noteworthy that viable cortical neurons showed no response to nanomolar concentrations of ouabain (Fig. 1, C and D). Treatment with 1 nM ouabain for 240 min did not induce any notable change in neuronal viability, as indicated both from the correlation analysis (Fig. 1C) and quantitative comparisons of the number of cells in each state (Fig. 1D). Therefore, in contrast to the effects of ouabain at concentrations exceeding 1 μ M, which causes large changes in ion balance and is known to be neurotoxic (Xiao et al., 2002), cultured cortical neurons were indifferent to the action of 1 nM ouabain.

Sustained exposure of neurons to GluR agonists is a neurotoxic insult that triggers necrosis and apoptosis. When neurons were exposed to 30 μ M NMDA for 240 min (30 μ M NMDA was always applied in combination with 30 μ M glycine, which is a coagonist of NMDARs; Johnson and Ascher, 1987), the treated neurons showed significantly fewer live cells (green) and more condensed apoptotic nuclei (orange) and necrotic (red) nuclei (Fig. 2A). A similar pattern of neu-

rotoxicity occurred when neurons were exposed to 30 μ M KA for 240 min (Fig. 2B). Therefore, cells exposed to chronic agonist exhibited significant apoptosis and necrosis, as expected. The green-red emission was highly colocalized (Fig. 2, C and D), indicating that apoptosis is the dominant mechanism of cell death in these neurons. Sustained exposure of neurons to either NMDA or KA caused a significant decrease in the number of viable neurons and a concomitant increase in the number of neurons undergoing cell apoptosis and cell death. These findings indicate that apoptosis plays a major role in the neurotoxicity produced by sustained exposure to GluR agonists.

Strikingly, this neurotoxicity can be prevented by including ouabain at 0.1 or 1 nM with the GluR agonists (Fig. 2, E and F). Neurons incubated with 30 μ M NMDA and 0.1 nM ouabain showed a viability comparable with the control conditions (Fig. 2E), without significant apoptosis. Even longer treatment with 30 μ M NMDA and 1 nM ouabain exceeding 360 min did not reveal the loss of neuronal viability. For instance, the obtained percentages of live, apoptotic, and necrotic neurons were 94 ± 1 , 2 ± 1 , and $4 \pm 1\%$ ($n = 9$), respectively, and were not significantly different from the control values ($p > 0.05$; ANOVA, post hoc Bonferroni test). A similar protective effect occurred when 30 μ M KA and 0.1 nM ouabain were simultaneously applied to neurons (Fig. 2F). The corresponding correlation plots (Fig. 2, G and H) show almost no colocalized fluorescence in the green and red spectral regions, indicating that the viable cells were not undergoing apoptosis.

From the average data for NMDA (Fig. 2I) and KA (Fig. 2J), it is apparent that long-term activation of both NMDARs and AMPAR/KARs induces excitotoxicity, in which the dominant mechanism of cell rundown is apoptosis. However, the inclusion of 0.1 or 1 nM ouabain with GluR agonists significantly decreased the quantity of apoptotic neurons and nearly doubled the number of viable neurons. The number of necrotic cells remained small and unchanged in both conditions and was comparable with values obtained under the control conditions (Fig. 1D). It should be noted that 0.01 nM ouabain was ineffective at preventing apoptosis. This result suggests that ouabain at subnanomolar concentrations (0.1–1 nM) actually increases cell viability during excitotoxic insult, by preventing the development of apoptosis.

To verify that the observed ouabain effects were mediated by Na⁺,K⁺-ATPase, digoxin, another highly specific ligand of the Na⁺,K⁺-ATPase cardiotonic steroids binding site (Katz et al., 2010), was also tested by using FVA. The incubation of neurons with 30 μ M NMDA and 1 nM digoxin for 240 min did not cause apoptosis. The average proportions of neurons found in these experiments were 73 ± 7 , 18 ± 3 , and $9 \pm 6\%$ ($n = 9$) for live, apoptotic, and necrotic cells, respectively. These data did not differ significantly from the values obtained in experiments with 30 μ M NMDA and 1 nM ouabain ($p > 0.05$; ANOVA, post hoc Bonferroni test). Therefore, 1 nM digoxin had similar antiapoptotic effects as 1 nM ouabain, suggesting that high-affinity binding of cardiotonic steroids to the Na⁺,K⁺-ATPase was indispensable for their antiapoptotic action.

Apoptosis induced by the activation of GluRs develops largely because of mitochondrial dysfunction (Green and Reed, 1998), although NMDARs and AMPAR/KARs trigger different apoptotic cascades (Wang et al., 2004). The endog-

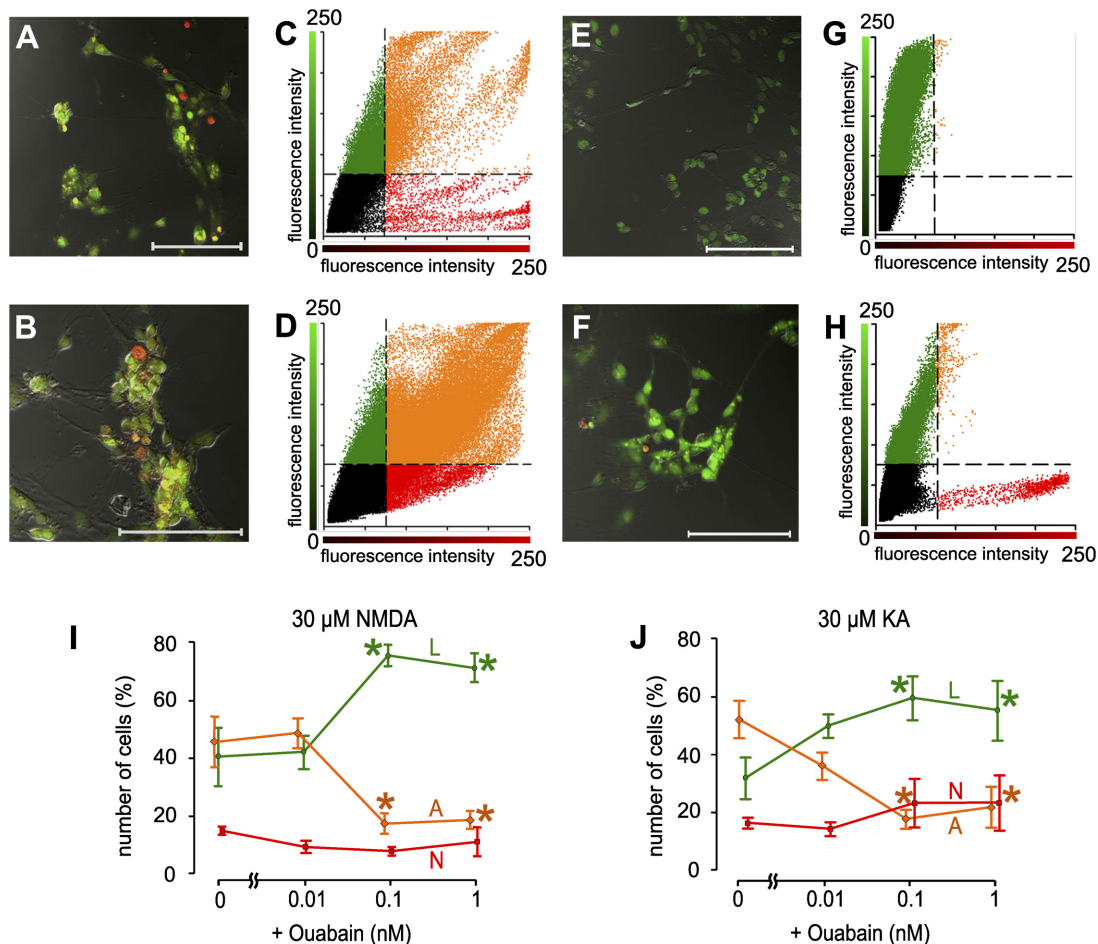


Fig. 2. Evaluation of neuroprotective, antiapoptotic action of 0.1 or 1 nM ouabain. A and B, the FVA images of neurons after 240-min treatment with 30 μ M NMDA (A) or 30 μ M KA (B). C and D, the correlation plots of images presented in A and B, respectively. Clearly, in addition to noncolocalized green and red fluorescence, large portions of fluorescence recorded in green and red spectral regions are colocalized, giving the orange color. This color pattern suggests that neurodegeneration develops by both necrosis and apoptosis. For the NMDA effects (A and C) the cell population consists of necrotic (7%), apoptotic (33%), and live (60%) neurons. For the KA effects (B and D) the cell population consists of necrotic (15%), apoptotic (59%), and live (26%) neurons. E and F, the FVA of neurons after 240-min treatment with 30 μ M NMDA (E) or 30 μ M KA (F) in the presence 0.1 nM ouabain. Scale bars in A, B, E, and F are 100 μ m. G, the correlation plot for the image obtained with NMDA (E). The fluorescence belongs to the green spectral region, suggesting that all neurons are alive. Cell viability is 100%. H, the correlation plot for the image obtained with KA (F). Whereas the largest portion of fluorescence belongs to the green spectral region, some fluorescence in the red spectral region also exists. The cell population consists of necrotic (2%), apoptotic (2%), and live (96%) neurons. The dashed lines in C, D, G, and H have the same meaning as in Fig. 1. I, quantitative comparisons of the data obtained with 30 μ M NMDA applied in the absence of ouabain and in combination with 0.01, 0.1, or 1 nM ouabain. The values for apoptotic and live neurons in the presence of either 0.1 or 1 nM ouabain differed significantly from the values obtained in 30 μ M NMDA in the absence and presence of 0.01 nM ouabain (*, $p < 0.0001$; ANOVA, post hoc Tukey's test; $n = 9-10$). J, quantitative comparisons of the data obtained with 30 μ M KA applied in the absence of ouabain and in combination with 0.01, 0.1, or 1 nM ouabain. The values for apoptotic and live neurons in the presence of either 0.1 or 1 nM ouabain differed significantly from the values obtained in 30 μ M KA in the absence and presence of 0.01 nM ouabain (*, $p < 0.0001$; ANOVA, post hoc Tukey's test; $n = 8-9$). In I and J, A, N, and L are the percentages of apoptotic, necrotic, and live neurons, respectively.

enous antiapoptotic protein Bcl-2 is an important regulator of mitochondrial function and energy metabolism and is involved in many vital cell processes. A decrease in Bcl-2 levels is routinely used as a marker of apoptosis (Adams and Cory, 1998). Because ouabain in our experiments selectively inhibited apoptosis, we further tested whether the expression level of Bcl-2 changed during NMDA- or KA- induced neurodegeneration. In control conditions, the majority of cortical neurons showed a high level of Bcl-2 immunostaining (Fig. 3, A and B). Subjecting these neurons to excitotoxic stress produced by 30 μ M KA (Fig. 3C) or 30 μ M NMDA (Fig. 3D) caused a significant decrease in Bcl-2 levels. However, coincubation of the GluR agonists with 0.1 or 1 nM ouabain completely prevented this effect (Fig. 3, E and F). The quantity of Bcl-2-positive neurons obtained after NMDA or KA alone was significantly lower than control values (Fig. 3G), but was

retained at near control values after combined application of NMDA or KA with ouabain (Fig. 3H). As in the case of FVA, experiments with 0.01 nM ouabain did not cause any change in the expression of Bcl-2. Thus, the measurement of Bcl-2 levels agreed well with the results obtained with FVA.

Concentration Dependence of Self-Neurotoxic Effect of Ouabain. We also tested the neurotoxic effects of ouabain in a wide range of concentrations from 1 nM to 30 μ M by using FVA. At 1 nM and below ouabain did not induce any changes in cell viability (Figs. 1 and 4). Sustained exposure (240 min) of neurons to 10 nM ouabain and above caused a significant decrease in the number of viable neurons (Fig. 4). In contrast to the effects of GluR agonists, the ouabain-induced cell rundown developed basically by necrosis, but not apoptosis. Our data are consistent with previous observations that neurons express the $\alpha 3$ -isoform of Na^+, K^+ -ATPase

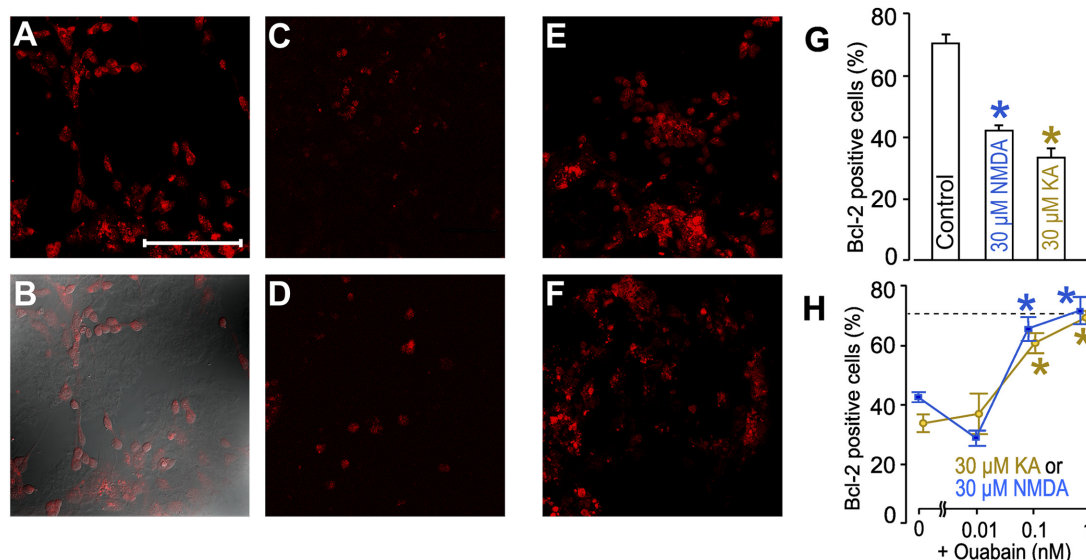


Fig. 3. Up-regulation of Bcl-2 expression during excitotoxic insults in the presence of 0.1 or 1 nM ouabain. A, Bcl-2 immunostaining of neurons under control conditions (incubation for 240 min in the bathing solution). Scale bar is 100 μm and valid for A to F. B, the same image as in A, combined with the transmitted light image (differential interference contrast). C, Bcl-2 immunostaining of neurons treated for 240 min with 30 μM KA. D, Bcl-2 immunostaining of neurons treated for 240 min with 30 μM NMDA. E, Bcl-2 immunostaining of neurons after exposure with 30 μM KA in the presence of 0.1 nM ouabain. F, Bcl-2 immunostaining of neurons after exposure with 30 μM NMDA in the presence of 1 nM ouabain. G, quantitative comparison of neurons expressing Bcl-2 under control and after excitotoxic insults. The values obtained after exposure with 30 μM NMDA or 30 μM KA differ significantly from the control value (*, $p < 0.0001$; ANOVA, post hoc Tukey's test; $n = 9$). H, quantitative comparisons of neurons expressing Bcl-2 after excitotoxic insults in the absence and presence of 0.01, 0.1, or 1 nM ouabain. The values obtained after exposure with 30 μM NMDA or 30 μM KA without ouabain and in the presence of 0.01 nM ouabain differ significantly from those in the presence of 0.1 and 1 nM ouabain ($p < 0.0001$; ANOVA, post hoc Tukey's test; $n = 9$). The dashed line indicates the mean value obtained under the control conditions.

whose enzymatic activity is already affected by 10 nM ouabain (Richards et al., 2007) and the mechanism of neuronal death corresponds to necrosis (Xiao et al., 2002).

Regulation of Intracellular Ca²⁺ Concentration by Ouabain. It is generally accepted that chronic neuronal depolarization followed by the free cytosolic Ca²⁺ concentration ([Ca²⁺]_i) increase initiates neuronal apoptosis during excitotoxic stress (Choi, 1988; Olney, 1994; Lipton, 1999; Khodorov, 2004). To investigate the possible mechanisms of neuroprotective, antiapoptotic action of subnanomolar ouabain concentrations, we undertook experiments in which whole-cell currents were recorded during long-lasting 30 μM NMDA or 30

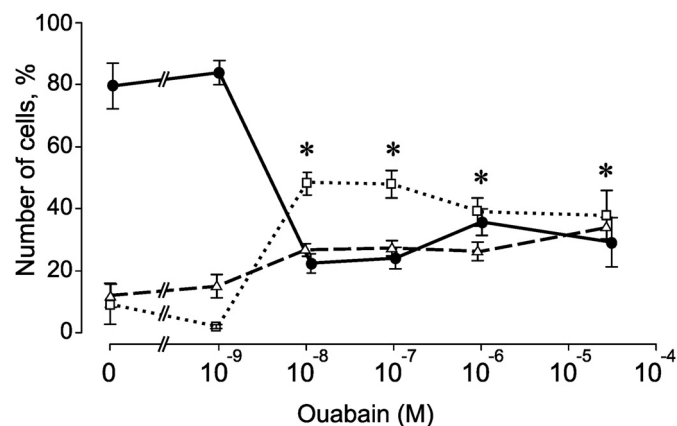


Fig. 4. Concentration dependence of ouabain neurotoxic effect. Quantitative comparisons of live (circles), necrotic (squares), and apoptotic (triangles) neurons after 240-min treatment with different ouabain concentrations. Each data point represents an average from four to nine experiments. The values for live and necrotic cells differ significantly from the corresponding values in 0 and 1 nM ouabain (*, $p < 0.001$; ANOVA, post hoc Tukey's test; $n = 9$).

μM KA applications and further studied the effects of subnanomolar ouabain by directly measuring intracellular Ca²⁺ signals using Fluo-3 or Fura-2. Both agonists caused the generation by neurons of inward currents that reveal a steady state (direct currents) as long as agonists were present (Fig. 5). Applications of 30 μM NMDA to neurons loaded with Fluo-3 (Fig. 6A) or Fura-2 (Fig. 6B) induced sustained intracellular Ca²⁺ responses lasting as long as NMDA was present. On average somatic free [Ca²⁺]_i under the control condition did not exceed 50 nM, whereas in the presence of NMDA it could reach 1 μM in our experiments. When 30 μM NMDA and 1 nM ouabain were applied simultaneously in experiments with either Fluo-3 (Fig. 6C) or Fura-2 (Fig. 6D) the Ca²⁺ response increased, but then declined in time gradually to almost the control value of [Ca²⁺]_i. The dynamics of NMDA-induced [Ca²⁺]_i increase in the absence and presence of 1 nM ouabain are compared in Fig. 6E. Obviously, 1 nM ouabain somehow stimulated intracellular Ca²⁺ buffering or extrusion of Ca²⁺ from neurons, resulting in decreased

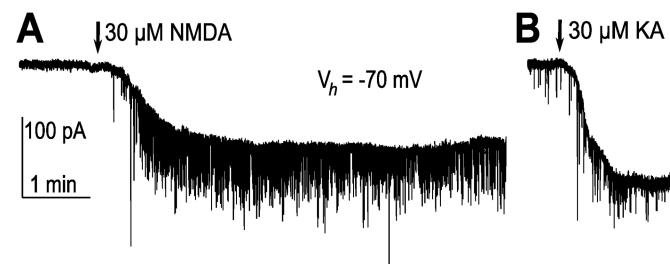


Fig. 5. Neuronal electrical activity during long-lasting GluR agonist applications. A, representative sweep of whole-cell currents illustrating neuronal responses to 30 μM NMDA application. B, representative sweep of whole-cell currents illustrating the response to 30 μM KA application. Agonist application is shown by the arrows.

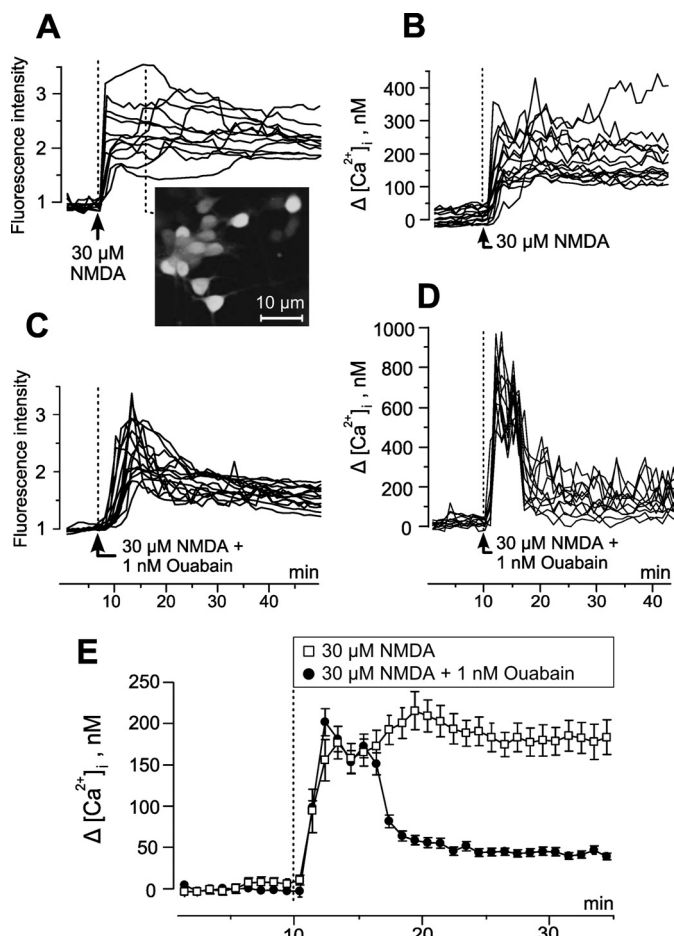


Fig. 6. Ouabain (1 nM) transforms the excessive sustained $[Ca^{2+}]_i$ increase induced by NMDA to a transient $[Ca^{2+}]_i$ response. **A**, sustained Ca^{2+} responses of neurons loaded with Fluo-3 on 30 μ M NMDA application (shown by the arrow). The inset illustrates neurons at the moment of fluorescence maximum indicated by the dashed line connected to the image. **B**, sustained increase of $[Ca^{2+}]_i$, measured in neurons loaded with Fura-2 in response to 30 μ M NMDA application (shown by the arrow). **C**, transient Ca^{2+} responses of neurons loaded with Fluo-3 on combined 30 μ M NMDA and 1 nM ouabain application (shown by the arrow). **D**, transient increase of $[Ca^{2+}]_i$, measured in neurons loaded with Fura-2 in response to combined 30 μ M NMDA and 1 nM ouabain application (shown by the arrow). In **A** to **D** data from single experiments are illustrated. **E**, the average dynamics of the $[Ca^{2+}]_i$ increases ($n = 5$; more than 60 neurons included in the statistics for each of the curves), measured in neurons loaded with Fura-2, reveal the capability of ouabain to eliminate the sustained $[Ca^{2+}]_i$ responses induced by NMDA. The protocol of applications and drug concentrations are shown above the plot. \square , data obtained with 30 μ M NMDA. \bullet , data obtained when 30 μ M NMDA was applied in combination with 1 nM ouabain.

$[Ca^{2+}]_i$. Perhaps, this process prevents an induction of apoptosis during excitotoxic insults.

Thus, Na^+,K^+ -ATPase is involved in the regulation of $[Ca^{2+}]_i$ during excitotoxic stress, suggesting that Ca^{2+} handling determines its neuroprotective antiapoptotic function.

Na^+,K^+ -ATPase Is Involved in the Regulation of Spontaneous Synaptic Activity through Intracellular Ca^{2+} -Dependent Mechanisms. In addition to the direct currents, GluR agonists induced considerable increases in sEPSC frequency, which were stably maintained at high levels in the presence of agonists (Figs. 5 and 7A). We were surprised to find that, when applied on top of 30 μ M NMDA or 30 μ M KA effects, 1 nM ouabain affected sEPSC with a delay of approximately 1 min (Fig. 7A), so the value of the

sEPSC frequency obtained either in NMDA (approximately 5 per s; Fig. 7B) or KA (approximately 1.2 per s; Fig. 7C) decreased to the value obtained under control conditions (approximately 0.3 per s; Fig. 7, B and C). Neither direct current amplitudes at -70 mV, nor I-V relationships of NMDA-activated (Fig. 7D) and KA-activated (Fig. 7E) integral currents were affected by 1 nM ouabain, suggesting the lack of its effect on NMDAR and AMPAR/KAR kinetics and conductance.

These data suggest that the increase of spontaneous synaptic activity in the neuronal network induced by GluR agonists may contribute in excitotoxicity via strengthening neuronal depolarization by endogenous glutamate. Ouabain at subnanomolar concentrations is able to recover sEPSC frequency to the control level.

In our experiments ouabain in the concentrations under study did not affect integral currents through NMDARs or ANPAR/KARs. We, therefore, verified the most prominent explanation of GluR agonists and ouabain effects on sEPSC frequency, suggesting that by interacting with presynaptic NMDARs and Na^+,K^+ -ATPase these compounds are involved in the regulation of presynaptic $[Ca^{2+}]_i$. Loading of neurons with BAPTA (2 and 5 μ M), a chelator of Ca^{2+} , to increase the capacity of intracellular Ca^{2+} buffering systems, eliminated both the NMDA effect (Fig. 7, F and G) and the ouabain effect on sEPSC frequency (Fig. 7G).

Na^+,K^+ -ATPase as a Signal Transducer Targeting the Plasma Membrane Na^+,Ca^{2+} Exchanger. A large body of evidence has accumulated suggesting that Na^+,K^+ -ATPase molecules are tightly packed with other integral proteins in functional clusters in the cell plasma membranes of different tissues. This provides direct molecule interplay and functional interaction between Na^+,K^+ -ATPase and neighboring proteins (Xie and Askari, 2002; Li and Xie, 2009). To look for the recipient of Na^+,K^+ -ATPase regulatory action in neurons we focused on the plasma membrane NCX, because it has been shown that these two molecules are anchored, forming a functional complex in the plasma membrane of cardiomyocytes (Xie and Askari, 2002; Aperia, 2007).

Experiments were performed in which the effects of 30 μ M NMDA and 1 nM ouabain were studied when 10 μ M 2-(2-(4-(4-nitrobenzyloxy)phenyl)ethyl)isothiourea methanesulfonate (KB-R7943) was present in the bathing solution. It is known that KB-R7943 at concentrations approximately 100 nM blocks the NCX in a reverse mode of transport (Iwamoto et al., 1996; Breder et al., 2000), whereas in concentrations used here both the forward and reverse transport were affected (Kimura et al., 1999; Breder et al., 2000). Inhibition of the NCX did not cause considerable changes in direct current amplitudes (Fig. 8A), but it did induce significant increase of sEPSC frequency (Fig. 8B; $p < 0.00033$, ANOVA, post hoc Tukey's test; $n = 12$). Application of 30 μ M NMDA caused a tremendous increase of sEPSC frequency, as in the experiments without KB-R7943 pretreatment (Fig. 8). In contrast to the ouabain effects obtained with active NCX, when the NCX was inhibited by KB-R7943, 1 nM ouabain failed to affect sEPSC frequency: it remained at the same high value as recorded in the presence of 30 μ M NMDA (Fig. 8).

In Ca^{2+} imaging experiments with Fura-2, combined application of 30 μ M NMDA and 1 nM ouabain caused temporal elevation of $[Ca^{2+}]_i$, but not Ca^{2+} overload (Fig. 6E). Adding

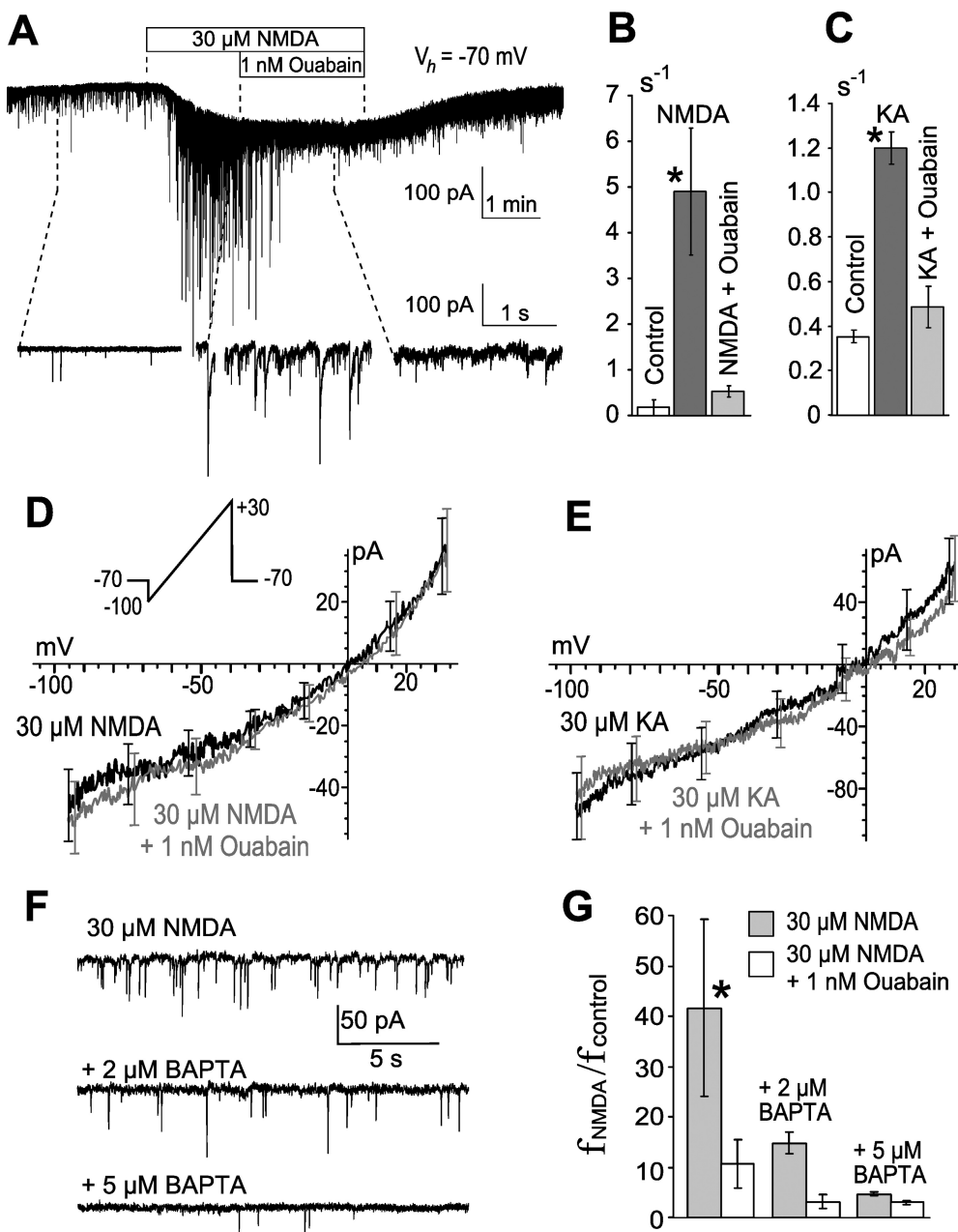


Fig. 7. Ouabain at 1 nM affects neuronal electrical activity induced by GluR agonists, lowering sEPSC frequency in an intracellular Ca²⁺-dependent manner. **A**, representative sweep of whole-cell currents illustrating neuronal responses to 30 μM NMDA applied alone and subsequently in combination with 1 nM ouabain. The protocol of application is indicated above the sweep. Traces below the whole-cell record are the sections (indicated by dashed lines) replotted at a higher time resolution to estimate the frequency of sEPSCs. **B** and **C**, quantitative comparisons of sEPSC frequencies under the control conditions, in the presence of 30 μM NMDA (**B**) or 30 μM KA (**C**) alone and with 1 nM ouabain. Values obtained in the presence of GluR agonists differ significantly from both the control value and those obtained in the presence of 1 nM ouabain (for NMDA, *, $p < 0.0003$, ANOVA, post hoc Tukey's test, $n = 5$; for KA, *, $p < 0.0003$, ANOVA, post hoc Tukey's test, $n = 5$), suggesting that 1 nM ouabain diminishes the sEPSC frequency increase produced with NMDA or KA. **D**, and **E**, I-V relationships of whole-cell direct currents induced by 30 μM NMDA (**D**) or 30 μM KA (**E**) alone and with the addition of 1 nM ouabain. For each of the I-V curves $n = 9$. Ramp protocol is shown in the inset of **D**. **F**, traces of whole-cell currents recorded in the presence of 30 μM NMDA on intact and loaded with 2 μM or 5 μM BAPTA neuronal cultures. **G**, histogram of sEPSC's relative frequencies ($f_{\text{NMDA}}/f_{\text{control}}$) obtained in the presence of 30 μM NMDA and with the addition of 1 nM ouabain on intact and loaded with 2 μM or 5 μM BAPTA neuronal cultures. The value obtained on intact cultures in the presence of 30 μM NMDA differs significantly from the rest of the data (*, $p < 0.004$; ANOVA, post hoc Tukey's test; $n = 8$). Loading with BAPTA of neurons eliminates both the sEPSC's frequency increase induced by NMDA and the effects of 1 nM ouabain.

10 μM KB-R7943 on the top of ouabain effect resulted in an uncompensated rise of [Ca²⁺]_i in neurons (Fig. 9A). Averaged data are shown in Fig. 9B. This observation demonstrates that the NCX under these particular conditions operates in a forward mode (removing Ca²⁺ from the cell) and is critically involved in intracellular Ca²⁺ regulation by ouabain.

Discussion

Our experiments disclose the antiapoptotic and neuroprotective effects of ultralow concentrations of ouabain and digoxin, which are manifested in the maintenance of the viability of the vast majority of cortical neurons during neurotoxic stress induced by long-lasting activation of NMDARs or AMPAR/KARs. It is well established that the GluR antagonists (2R)-amino-5-phosphonopentanoate, a selective antagonist of NMDARs, and 6-cyano-7-nitroquinoxaline-2,3-dione, a selective antagonist of AMPA/KARs (Traynelis et al., 2010),

exhibit neuroprotective effects by blocking receptors that trigger excitotoxicity, thereby preventing the development of both necrosis and apoptosis (Choi, 1988; Olney, 1994; Lipton, 1999; Mironova et al., 2007). In contrast, subnanomolar concentrations of ouabain or digoxin in our experiments inhibited only apoptosis (Fig. 2). Normal expression levels of the antiapoptotic protein Bcl-2 were found in the presence of ouabain compared with decreased levels observed after NMDA- or KA-induced neurotoxic stress (Fig. 3). This observation suggests that ouabain and digoxin, which interacts with the highly conserved cardiotonic receptor of Na⁺,K⁺-ATPase, can somehow stimulate antiapoptotic intracellular pathways. Because ouabain and digoxin inhibit Na⁺,K⁺-ATPase of rats at concentrations (Fig. 4) that significantly exceed (Sweadner, 1989; Xiao et al., 2002; Richards et al., 2007; Katz et al., 2010) those that are antiapoptotic (0.01–1 nM), one may speculate that their neuroprotective effect could be

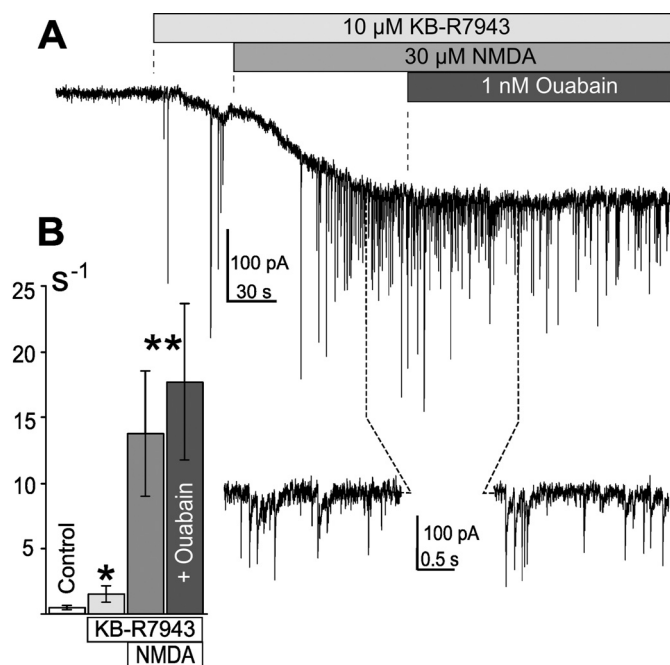


Fig. 8. Inhibition of the plasma membrane $\text{Na}^+, \text{Ca}^{2+}$ exchanger abolishes the effect of 1 nM ouabain on sEPSC frequency. **A**, representative sweep of whole-cell currents illustrating neuronal responses to 30 μM NMDA alone and in combination with 1 nM ouabain during treatment with an inhibitor of the plasma membrane $\text{Na}^+, \text{Ca}^{2+}$ exchanger (KB-R7943). The protocol of applications and drug concentrations are shown above the sweep. Traces below the record are the sections (indicated by dashed lines) replotted at a higher time resolution. **B**, quantitative comparisons of sEPSC frequencies obtained in the presence of 30 μM NMDA alone and with 1 nM ouabain in the course of treatment with KB-R7943. The value obtained in the presence of 10 μM KB-R7943 differ significantly from the control value (*, $p < 0.0033$; ANOVA, post hoc Tukey's test; $n = 12$); data obtained in the presence of 30 μM NMDA (either alone or with 1 nM ouabain) differ significantly from those obtained before NMDA application (**, $p < 0.0033$; ANOVA, post hoc Tukey's test; $n = 12$).

realized because of a signaling function of the cardiotonic receptor on Na^+, K^+ -ATPase. The evaluation of the high-affinity binding state for ouabain with the equilibrium dissociation constant of approximately 1 nM in the crystal structure of Na^+, K^+ -ATPase (Ogawa et al., 2009) supports this assumption.

To provide some clues in favor of the mechanism of the ouabain antiapoptotic effects, whole-cell patch-clamp records during long-lasting NMDA or KA presence in the chamber were performed. These conditions were similar to our excito-

toxic insult experiments. When NMDA or KA was applied, neurons generated inward direct currents through the channels of activated NMDARs and AMPA/KARs, respectively (Fig. 5). Cultured cortical neurons express mRNA encoding the NR1, NR2A, and NR2B subunits of NMDARs (Zhong et al., 1994). Because the channels of NR1/NR2A and NR1/NR2B subunit compositions are highly permeable for Ca^{2+} (Traynelis et al., 2010), some fraction of direct currents is determined by the Ca^{2+} entry into neurons, resulting in an immediate, continued elevation of $[\text{Ca}^{2+}]_i$ (Fig. 6, A and B) (MacDermott et al., 1986). In the case of AMPA/KARs the intracellular Ca^{2+} signal has a more complex nature and is determined by expression of the GluR2 subunit of AMPARs, which rules the Ca^{2+} permeability of their channels (Burnashev et al., 1992; Traynelis et al., 2010). Cultured cortical neurons reveal a variety of intracellular Ca^{2+} response kinetics after KA applications (Abushik et al., 2011). The intracellular Ca^{2+} signal and further delayed intracellular Ca^{2+} deregulation (Khodorov, 2004) is thought to trigger neuronal apoptosis. Considering the high Ca^{2+} permeability of NMDARs and GluR2 lacking AMPARs, the most plausible way to antagonize apoptosis would be an influence on channel open probability, kinetics, or conductance, which would eliminate Ca^{2+} entry in the cytoplasm. GluR antagonists (Khodorov, 2004; Mironova et al., 2007; Traynelis et al., 2010) and channel blockers, (+)-5-methyl-10,11-dihydro-5H-dibenzo[*a,d*]cyclohepten-5,10-imine (MK-801), ketamine, memantine, etc. (Church et al., 1988; Antonov et al., 1995, 1998; Lipton, 1999; Traynelis et al., 2010) represent examples of such an influence. In our experiments no effects of ouabain at antiapoptotic concentrations (0.1 and 1 nM) either on the amplitude (Fig. 7A) or I-V relationship of direct currents transmitted through open NMDARs (Fig. 7D) or AMPA/KARs (Fig. 7E) were found. The lack of effects may suggest that the target of ouabain regulation is located downstream of the Ca^{2+} entry into neurons.

A growing body of evidence is accumulating showing that NMDARs, AMPARs, and KARs are expressed in presynaptic terminals, as well as in postsynaptic membranes (for review see Pinheiro and Mulle, 2008). These autoreceptors play a role in synaptic plasticity, providing either a potentiation or depression of EPSC and spontaneous transmitter release in different brain structures. Several forms of synaptic plasticity were also demonstrated in primary cultures of rat cortical neurons (Han and Stevens, 2009). In addition to direct cur-

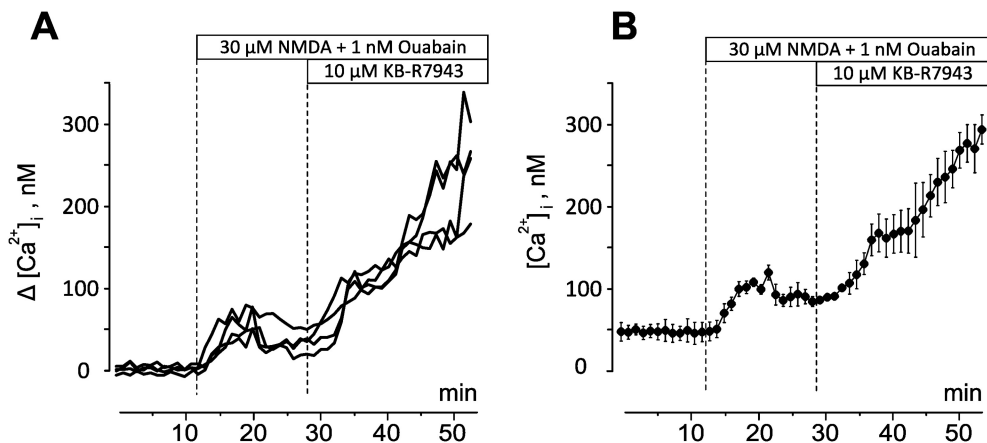


Fig. 9. Inhibition of the plasma membrane $\text{Na}^+, \text{Ca}^{2+}$ exchanger revokes the effect of 1 nM ouabain on intracellular Ca^{2+} . **A**, intracellular Ca^{2+} responses measured in neurons loaded with Fura-2 on simultaneous 30 μM NMDA and 1 nM ouabain application, followed by the addition of 10 μM KB-R7943. **B**, the average $[\text{Ca}^{2+}]_i$ dynamics ($n = 3$; more than 20 neurons included in the statistics), measured in neurons loaded with Fura-2. KB-R7943 abolishes the ouabain-induced $[\text{Ca}^{2+}]_i$ decrease. The protocol of applications and drug concentrations are shown above the traces.

rents in the presence of NMDA and KA, a tremendous increase of sEPSC frequency (Figs. 5 and 7, A-C) was observed. To keep the conditions of experiments similar to those in the excitotoxicity study we did not add tetrodotoxin, a blocker of voltage-gated Na⁺ channels, and bicuculline, an inhibitor of ligand-gated γ -aminobutyric acid type A receptors, in the bathing solution. Synaptic currents recorded under these particular conditions had different origins. Obviously, some giant sEPSCs appeared that, perhaps, represented EPSCs evoked by presynaptic neuron spike firing enforced by chronic neuronal depolarization in the network. sEPSCs of smaller amplitude may have represented miniature EPSCs. Some contribution of inhibitory currents was also possible. Overall, the antiapoptotic ouabain concentrations applied on top of the agonist effects abolished the increase of sEPSC frequency (Fig. 7A), which returned to the control value (Fig. 7, B and C). Clearly, loading neurons with BAPTA, a chelator of Ca²⁺, to extend the intracellular Ca²⁺ buffering capacity abolished both the NMDA-induced sEPSC discharge and the compensatory effects of ouabain (Fig. 7, F and G). This may suggest that the NMDA-induced sEPSC discharge is caused by the accumulation of Ca²⁺ in presynaptic boutons, whereas ouabain at antiapoptotic concentrations somehow up-regulates intracellular Ca²⁺ clearance processes. Therefore, the binding of ouabain to Na⁺,K⁺-ATPase may contribute to the regulation of presynaptic [Ca²⁺]_i. Direct measurements of intracellular Ca²⁺ dynamics and concentration supported the conclusion drawn from the experiments described above. Whereas applications of NMDA to neurons caused the immediate, continuous elevation of [Ca²⁺]_i (Fig. 6, A and B), combined applications of NMDA with 1 nM ouabain induced a transient rise of [Ca²⁺]_i to a maximum reaching 1 μ M in some neurons, which then declined gradually in time (Fig. 6, C and D). In 10 min the [Ca²⁺]_i recovered to the control values (Fig. 6E). These results are consistent with the data obtained by using the patch-clamp technique and support the assumption that Na⁺,K⁺-ATPase is involved in the regulation of [Ca²⁺]_i. Clearly, voltage-gated Ca²⁺ channels as an alternative to GluR way of Ca²⁺ entry (AWCE) could play a role in ouabain action. However, we did not find any effects of antiapoptotic ouabain concentrations on neuronal I-V relationships under the control conditions (data not shown). Therefore, ouabain-induced Ca²⁺ clearance most likely is determined by up-regulation of Ca²⁺ extrusion rather than inhibition of Ca²⁺ entry.

In neurons, Ca²⁺ extrusion is operated by the plasma membrane Ca²⁺ pump and Na⁺,Ca²⁺ exchangers. The plasma membrane Ca²⁺ pump has high Ca²⁺ affinity but low transport capacity, whereas the NCX has a low affinity, but a higher capacity to transport Ca²⁺ (Bano et al., 2005). Inhibition of Ca²⁺ efflux from cells by the NCX is sufficient to cause sustained intracellular Ca²⁺ elevation and the demise of neurons. The expression of the NCX prevented Ca²⁺ overload and rescued neurons from excitotoxic death (Bano et al., 2005). Treatment of cortical neurons with a specific inhibitor of the NCX, KB-R7943 (Iwamoto et al., 1996; Breder et al., 2000), in our experiments prevented the compensatory effects of ouabain, which lost the ability to decrease [Ca²⁺]_i (Fig. 9) and the sEPSC frequency in the NMDA-induced sEPSC discharge (Fig. 8). Known KB-R7943 side effects (partial inhibition NMDAR and L-type Ca²⁺ channels; Brus-

tovetsky et al., 2011) should oppose intracellular Ca²⁺ accumulation that was not observed in our experiments. Therefore, this observation could be interpreted in a way that the NCX is the most likely candidate as a molecular target for Na⁺,K⁺-ATPase signal regulation. This functional interaction of the ouabain liganded Na⁺,K⁺-ATPase with the NCX somehow enforces Ca²⁺ extrusion and protects neurons from Ca²⁺ overload. Our conclusion is consistent with a previous study on snail neurons, which demonstrated a stimulation of the plasma membrane Na⁺,Ca²⁺ exchange by nanomolar concentrations of ouabain (Saghian et al., 1996). In those experimental conditions, however, the reversed mode of transport was up-regulated, causing intracellular Ca²⁺ accumulation. Presumably, these effects are induced by nondirect ouabain action on the NCX and may be secondary to a rise of intracellular cAMP (Saghian et al., 1996). Because Na⁺,K⁺-ATPase is the only known, highly specific receptor for ouabain and other cardiotonic steroids (Ogawa et al., 2009; Lingrel, 2010), it is unlikely that ouabain directly interacts with the NCX. In our experiments another specific ligand of the Na⁺,K⁺-ATPase cardiotonic steroid binding site, digoxin, reveals antiapoptotic action as well as ouabain. This corroborates our assumption that it is Na⁺,K⁺-ATPase that is a primary target triggering neuroprotection.

The interpretation of our data is illustrated in Fig. 10. Under normal conditions the capacity of intracellular Ca²⁺ buffering systems and Ca²⁺ extrusion by the NCX are sufficient to compensate Ca²⁺ that enter neurons through the AWCE representing different types of voltage-gated Ca²⁺ channels and pumps (Fig. 10A). The activation of autosynaptic and postsynaptic GluRs (in Fig. 10 only NMDARs are shown in presynaptic terminals for simplicity) causes depolarization and additional Ca²⁺ entry through the channels of NMDARs and AWCE, resulting in Ca²⁺ overload (Fig. 10B). In addition, the accumulation of free Ca²⁺ in presynaptic boutons elevates the probability of spontaneous vesicular transmitter release increasing sEPSC frequency. The occupation by ouabain of its binding site on Na⁺,K⁺-ATPase is followed by an acceleration of Ca²⁺ extrusion by the NCX (Fig. 10C). This prevents Ca²⁺ accumulation in cytoplasm. Inhibition of the NCX eliminates Ca²⁺ extrusion from neurons resulting in further Ca²⁺ overload, which makes ouabain binding ineffective (Fig. 10D). Whether those functional interactions between Na⁺,K⁺-ATPase and the NCX include direct molecular interactions remains to be elucidated.

The range of ouabain antiapoptotic concentrations corresponds well with the endogenous ouabain level, which varies from 0.1 to 0.74 nM in rat blood plasma and cerebrospinal fluid (Dobretsov and Stimers, 2005). Similar antiapoptotic effects of low ouabain doses have been shown to be associated with enhanced production of Bcl-2 in another neurodegeneration model when KA and ouabain were injected in the brain *in vivo* (Golden and Martin, 2006). Both findings provide corroborating evidence for the physiological relevance of endogenous ouabain. Thus, the data presented here demonstrate a novel function of Na⁺,K⁺-ATPase as a neuroprotective molecule that might be triggered by binding of endogenous ouabain or its analogs to a highly conserved cardiotonic/ouabain receptor site.

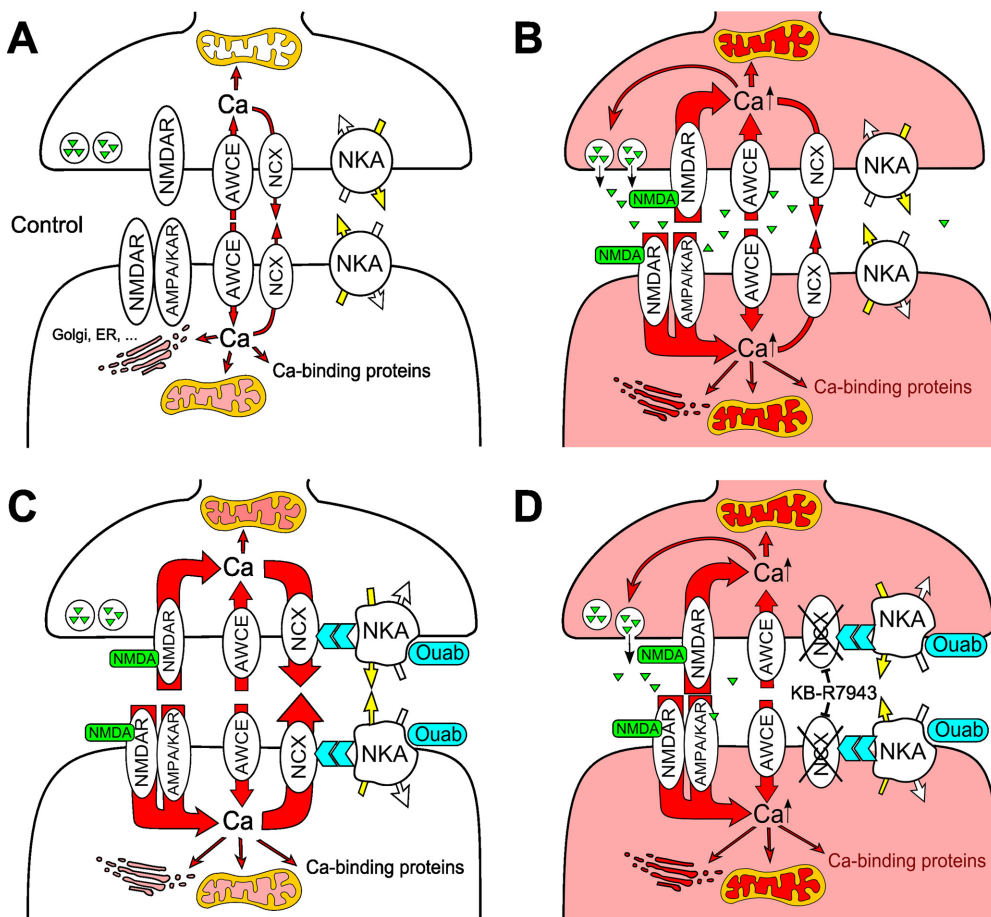


Fig. 10. Schematics of data interpretation. A, control conditions, when Ca^{2+} entry in neurons and presynaptic terminals is compensated by intracellular buffering systems and Ca^{2+} extrusion by the NCX. B, NMDA activates autosynaptic and postsynaptic NMDARs and causes Ca^{2+} overload, resulting in an increase in sEPSC frequency. C, ouabain occupation of the binding site on Na^+, K^+ -ATPase accelerates Ca^{2+} extrusion, influencing the NCX that prevents neurons from Ca^{2+} overload. D, the inhibition of the NCX abolishes the neuroprotective effects of ouabain, because it prevents Ca^{2+} extrusion and induces Ca^{2+} overload. NKA is Na^+, K^+ -ATPase, and Ouab is ouabain molecule. Triangles are glutamate molecules, and other symbols have their usual meanings. Golgi apparatus, endoplasmic reticulum, and mitochondria are shown as Ca^{2+} buffering systems. For further explanation see *Discussion*.

Acknowledgments

We thank Dr. J. W. Johnson and Dr. J. A. Heiny for reading the manuscript and providing critical suggestions.

Authorship Contributions

Participated in research design: Krivoi and Antonov.
Conducted experiments: Sibarov, Bolshakov, Abushik, and Antonov.
Performed data analysis: Sibarov, Bolshakov, Abushik, and Antonov.
Wrote or contributed to the writing of the manuscript: Krivoi and Antonov.

References

- Abushik PA, Bolshakov AE, Sibarov DA, and Antonov SM (2011) Mechanisms of heterogeneity of calcium response to kainate and neuronal types in rat cortical primary culture. *Biochemistry (Moscow)* **5**:92–100.
 Adams JM and Cory S (1998) The Bcl-2 protein family: arbiters of cell survival. *Science* **281**:1322–1326.
 Antonov SM, Gmiro VE, and Johnson JW (1998) Binding sites for permeant ions in the channel of NMDA receptors and their effects on channel block. *Nat Neurosci* **1**:451–461.
 Antonov SM, Johnson JW, Lukomskaia NY, Potapyeva NN, Gmiro VE, and Magazanik LG (1995) Novel adamantane derivatives act as blockers of open ligand-gated channels and as anticonvulsants. *Mol Pharmacol* **47**:558–567.
 Aperia A (2007) New roles for an old enzyme: Na, K -ATPase emerges as an interesting drug target. *J Intern Med* **261**:44–52.
 Bagrov AY and Shapiro JI (2008) Endogenous digitalis: pathophysiologic roles and therapeutic applications. *Nat Clin Pract Nephrol* **4**:378–392.
 Bano D, Young KW, Guerin CJ, Lefevre R, Rothwell NJ, Naldini L, Rizzuto R, Carafoli E, and Nicotera P (2005) Cleavage of the plasma membrane $\text{Na}^+/\text{Ca}^{2+}$ exchanger in excitotoxicity. *Cell* **120**:275–285.
 Blaustein MP (1993) Physiological effects of endogenous ouabain: control of intracellular Ca^{2+} stores and cell responsiveness. *Am J Physiol Cell Physiol* **264**:C1367–C1387.
 Bliss TV and Collingridge GL (1993) A synaptic model of memory: long-term potentiation in the hippocampus. *Nature* **361**:31–39.
 Breder J, Sabelhaus CF, Opitz T, Reymann KG, and Schröder UH (2000) Inhibition

- of different pathways influencing Na^+ homeostasis protects organotypic hippocampal slice cultures from hypoxic/hypoglycemic injury. *Neuropharmacology* **39**:1779–1787.
 Brustovetsky T, Brittain MK, Sheets PL, Cummins TR, Pinelis V, and Brustovetsky N (2011) KB-R7943, an inhibitor of the reverse $\text{Na}^+/\text{Ca}^{2+}$ exchanger, blocks N-methyl-D-aspartate receptor and inhibits mitochondrial complex I. *Br J Pharmacol* **162**:255–270.
 Burnashev N, Monyer H, Seeburg PH, and Sakmann B (1992) Divalent ion permeability of AMPA receptor channels is dominated by the edited form of a single subunit. *Neuron* **8**:189–198.
 Choi DW (1987) Ionic dependence of glutamate neurotoxicity. *J Neurosci* **7**:369–379.
 Choi DW (1988) Glutamate neurotoxicity and diseases of the nervous system. *Neuron* **1**:623–634.
 Church J, Zeman S, and Lodge D (1988) The neuroprotective action of ketamine and MK-801 after transient cerebral ischemia in rats. *Anesthesiology* **69**:702–709.
 Desfrere L, Karlsson M, Hiyoshi H, Malmersjö S, Nanou E, Estrada M, Miyakawa A, Lagercrantz H, El Manira A, Lal M, et al. (2009) Na, K -ATPase signal transduction triggers CREB activation and dendritic growth. *Proc Natl Acad Sci U S A* **106**:2212–2217.
 Dobretsov M and Stimers JR (2005) Neuronal function and $\alpha 3$ isoform of the Na/K -ATPase. *Front Biosci* **10**:2373–2396.
 Golden WC and Martin LJ (2006) Low-dose ouabain protects against excitotoxic apoptosis and up-regulates nuclear Bcl-2 in vivo. *Neuroscience* **137**:133–144.
 Green DR and Reed JC (1998) Mitochondria and apoptosis. *Science* **281**:1309–1312.
 Han EB and Stevens CF (2009) Development regulates a switch between post- and presynaptic strengthening in response to activity deprivation. *Proc Natl Acad Sci U S A* **106**:10817–10822.
 Hazelwood LA, Free RB, Cabrera DM, Skinbjerg M, and Sibley DR (2008) Reciprocal modulation of function between the D1 and D2 dopamine receptors and the Na^+, K^+ -ATPase. *J Biol Chem* **283**:36441–36453.
 Heiny JA, Kravtsova VV, Mandel F, Radzyukevich TL, Benziane B, Prokofiev AV, Pedersen SE, Chibalin AV, and Krivoi II (2010) The nicotinic acetylcholine receptor and the Na, K -ATPase $\alpha 2$ isoform interact to regulate membrane electrogenesis in skeletal muscle. *J Biol Chem* **285**:28614–28626.
 Iwamoto T, Watano T, and Shigekawa M (1996) A novel isothiourea derivative selectively inhibits the reverse mode of $\text{Na}^+, \text{Ca}^{2+}$ exchange in cells expressing NCX1. *J Biol Chem* **271**:22391–22397.
 Iwasato T, Datwani A, Wolf AM, Nishiyama H, Taguchi Y, Tonegawa S, Knöpfel T, Erzurumlu RS, and Itoharu S (2000) Cortex-restricted disruption of NMDAR1 impairs neuronal patterns in the barrel cortex. *Nature* **406**:726–731.
 Johnson JW and Ascher P (1987) Glycine potentiates the NMDA response in cultured mouse brain neurons. *Nature* **325**:529–531.

- Johnston MV (1994) Neuronal death in development, aging, and disease. *Neurobiol Aging* **15**:235–236.
- Katz A, Lifshitz Y, Bab-Dinitz E, Kapri-Pardes E, Goldshleger R, Tal DM, and Karlish SJ (2010) Selectivity of digitalis glycosides for isoforms of human Na,K-ATPase. *J Biol Chem* **285**:19582–19592.
- Khodorov B (2004) Glutamate-induced deregulation of calcium homeostasis and mitochondrial dysfunction in mammalian central neurones. *Prog Biophys Mol Biol* **86**:279–351.
- Kidd VJ (1998) Proteolytic activities that mediate apoptosis. *Annu Rev Physiol* **60**:533–573.
- Kimura J, Watano T, Kawahara M, Sakai E, and Yatabe J (1999) Direction-independent block of bi-directional Na⁺/Ca²⁺ exchange current by KB-R7943 in guinea-pig cardiac myocytes. *Br J Pharmacol* **128**:969–974.
- Krivoi II, Drabkina TM, Kravtsova VV, Vasiliev AN, Eaton MJ, Skatchkov SN, and Mandel F (2006) On the functional interaction between nicotinic acetylcholine receptor and Na⁺,K⁺-ATPase. *Pflugers Arch* **452**:756–765.
- Li Z and Xie Z (2009) The Na/K-ATPase/Src complex and cardiotoxic steroid-activated protein kinase cascades. *Pflugers Arch* **457**:635–644.
- Lingrel JB (2010) The physiological significance of the cardiotoxic steroid/ouabain-binding site of the Na,K-ATPase. *Annu Rev Physiol* **72**:395–412.
- Lipton P (1999) Ischemic cell death in brain neurons. *Physiol Rev* **79**:1431–1568.
- MacDermott AB, Mayer ML, Westbrook GL, Smith SJ, and Barker JL (1986) NMDA-receptor activation increases cytoplasmic calcium concentration in cultured spinal cord neurones. *Nature* **321**:519–522.
- Mironova EV, Evstratova AA, and Antonov SM (2007) A fluorescence vital assay for the recognition and quantification of excitotoxic cell death by necrosis and apoptosis using confocal microscopy on neurons in culture. *J Neurosci Methods* **163**:1–8.
- Nowak L, Bregestovski P, Ascher P, Herbet A, and Prochiantz A (1984) Magnesium gates glutamate-activated channels in mouse central neurones. *Nature* **307**:462–465.
- Ogawa H, Shinoda T, Cornelius F, and Toyoshima C (2009) Crystal structure of the sodium-potassium pump (Na⁺,K⁺-ATPase) with bound potassium and ouabain. *Proc Natl Acad Sci U S A* **106**:13742–13747.
- Olney JW (1994) Excitatory transmitter neurotoxicity. *Neurobiol Aging* **15**:259–260.
- Pinheiro PS and Mulle C (2008) Presynaptic glutamate receptors: physiological functions and mechanisms of action. *Nat Rev Neurosci* **9**:423–436.
- Radzyukevich TL, Lingrel JB, and Heiny JA (2009) The cardiac glycoside binding site on the Na,K-ATPase α 2 isoform plays a role in the dynamic regulation of active transport in skeletal muscle. *Proc Natl Acad Sci U S A* **106**:2565–2570.
- Richards KS, Bommert K, Szabo G, and Miles R (2007) Differential expression of Na⁺/K⁺-ATPase α -subunits in mouse hippocampal interneurons and pyramidal cells. *J Physiol* **585**:491–505.
- Rose EM, Koo JC, Antflick JE, Ahmed SM, Angers S, and Hampson DR (2009) Glutamate transporter coupling to Na,K-ATPase. *J Neurosci* **29**:8143–8155.
- Rossi DJ, Oshima T, and Attwell D (2000) Glutamate release in severe brain ischemia is mainly by reversed uptake. *Nature* **403**:316–321.
- Saghian AA, Ayrapetyan SN, and Carpenter DO (1996) Low concentrations of ouabain stimulate Na/Ca exchange in neurons. *Cell Mol Neurobiol* **16**:489–498.
- Schoner W and Scheiner-Bobis G (2007) Endogenous and exogenous cardiac glycosides and their mechanisms of action. *Am J Cardiovasc Drugs* **7**:173–189.
- Sweadner KJ (1989) Isozymes of the Na⁺/K⁺-ATPase. *Biochim Biophys Acta* **988**:185–220.
- Tang YP, Shimizu E, Dube GR, Rampon C, Kerchner GA, Zhuo M, Liu G, and Tsien JZ (1999) Genetic enhancement of learning and memory in mice. *Nature* **401**:63–69.
- Traynelis SF, Wollmuth LP, McBain CJ, Menniti FS, Vance KM, Ogden KK, Hansen KB, Yuan H, Myers SJ, and Dingledine R (2010) Glutamate receptor ion channels: structure, regulation, and function. *Pharmacol Rev* **62**:405–496.
- Wang H, Yu SW, Koh DW, Lew J, Coombs C, Bowers W, Federoff HJ, Poirier GG, Dawson TM, and Dawson VL (2004) Apoptosis-inducing factor substitutes for caspase executioners in NMDA-triggered excitotoxic neuronal death. *J Neurosci* **24**:10963–10973.
- Xiao AY, Wei L, Xia S, Rothman S, and Yu SP (2002) Ionic mechanism of ouabain-induced concurrent apoptosis and necrosis in individual cultured cortical neurons. *J Neurosci* **22**:1350–1362.
- Xie Z and Askari A (2002) Na⁺/K⁺-ATPase as a signal transducer. *Eur J Biochem* **269**:2434–2439.
- Zelenin AV (1966) Fluorescence microscopy of lysosomes and related structures in living cells. *Nature* **212**:425–426.
- Zhong J, Russell SL, Pritchett DB, Molinoff PB, and Williams K (1994) Expression of mRNA encoding subunits of the N-methyl-D-aspartate receptor in cultured cortical neurons. *Mol Pharmacol* **45**:846–853.

Address correspondence to: Sergei M. Antonov, Sechenov Institute of Evolutionary Physiology and Biochemistry, Russian Academy of Sciences, Torez pr. 44, St. Petersburg, 194223, Russia. E-mail: antonov452002@yahoo.com